Supplementary Figure 1

A

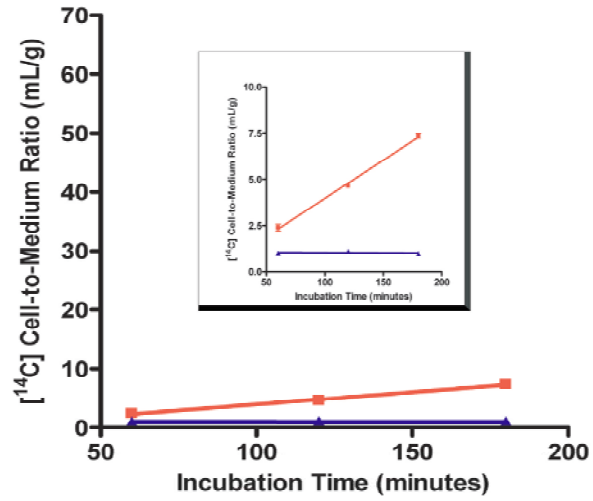

C

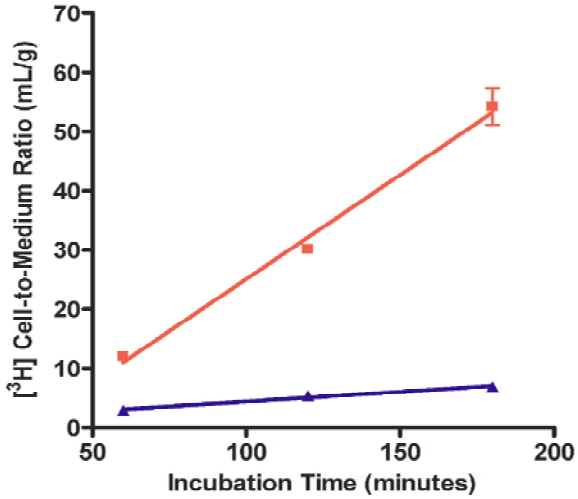

B

Cell Line	[^{14}C] C/M Ratio (Mean ± SEM, mL·g^{-1})			Regression Eqn.
	@ 60 min.	*@ 120 min.*	*@ 180 min.*	
CD-UPRT^{-}	1.003 ± 0.022	1.093 ± 0.064	0.973 ± 0.126	y = 1.053 + 0.0002x
CD-UPRT^{+}	2.380± 0.195	4.463 ± 0.085	7.347 ± 0.140	y = -0.177 + 0.0414x

D

Cell Line	[^{3}H] C/M Ratio (Mean ± SEM, mL·g^{-1})			Regression Eqn.
	@ 60 min.	*@ 120 min.*	*@ 180 min.*	
CD-UPRT^{-}	2.923 ± 0.039	5.427 ± 0.402	6.930 ± 0.116	y = 1.087 + 0.0334x
CD-UPRT^{+}	12.007 ± 0.278	30.103 ± 0.808	54.173 ± 3.096	y = -10.07 + 0.3514x

Supplementary Figure 2

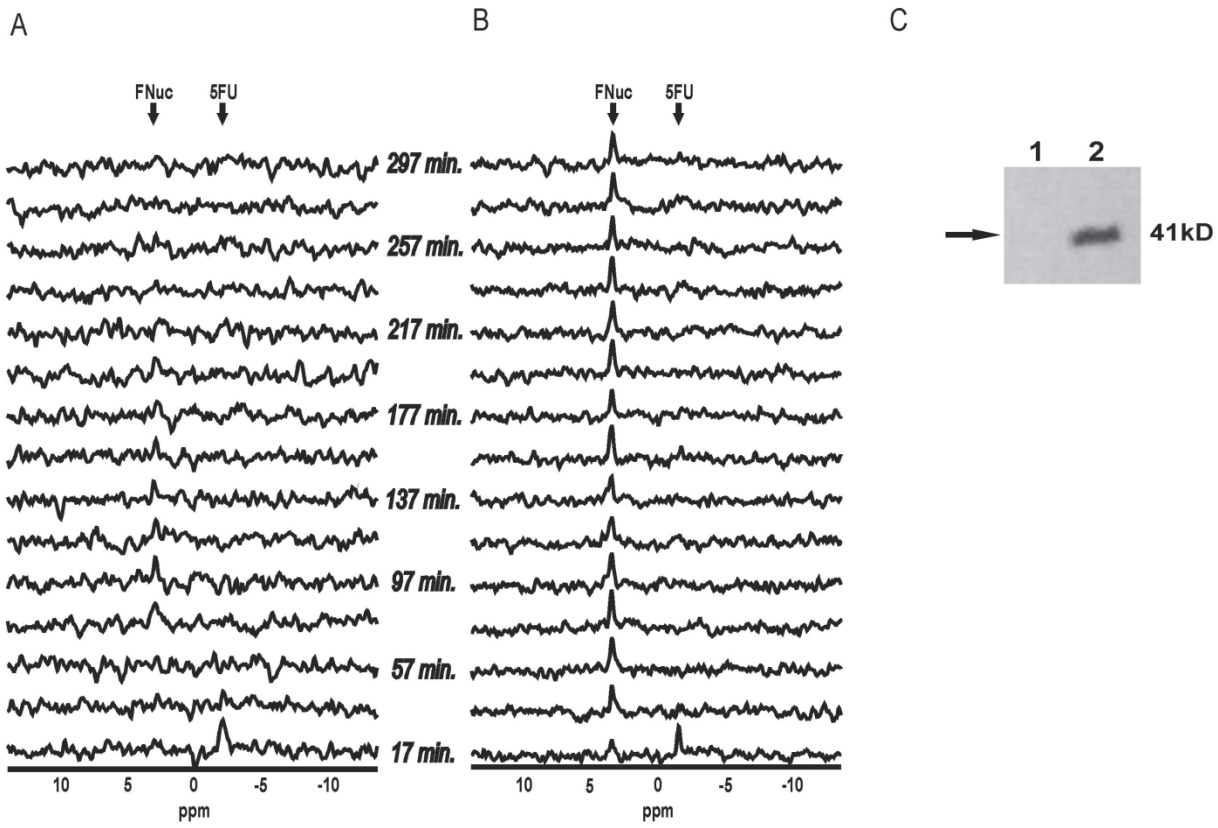

Supplementary Figure 3

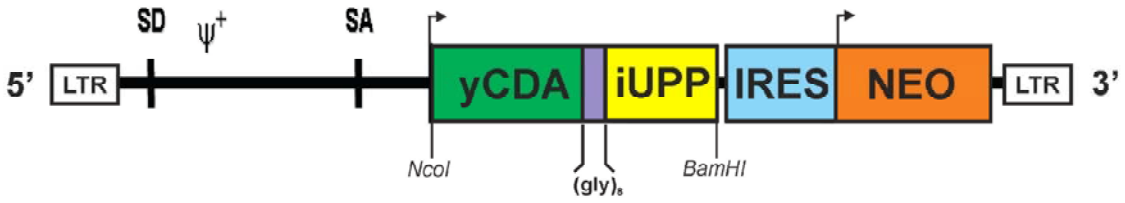

Supplementary Figure 4

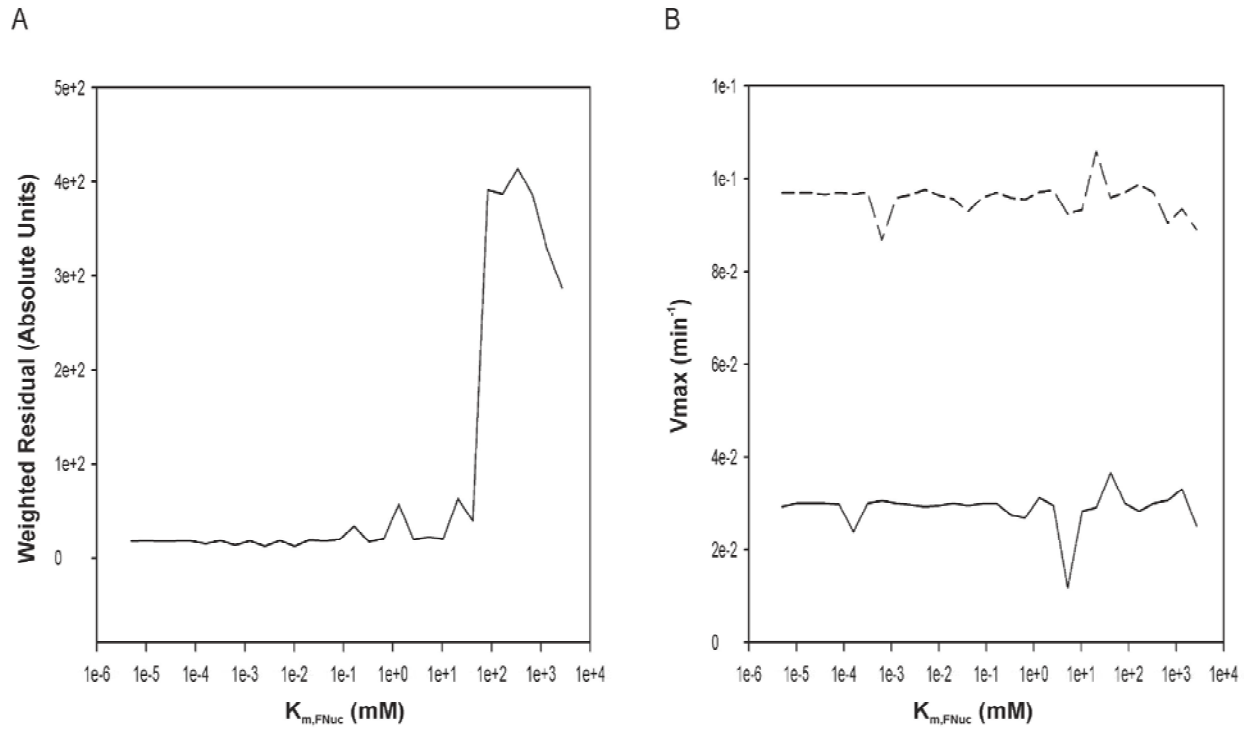

Supplementary Figure 1. Probe efficiency was compared in radiouptake studies using (a) [^{14}C]-5FC (with enlarged inset) and (b) [^{3}H]-5FU. The amount of accumulated radioactivity in CD-UPRT+ (■) and CD-UPRT- (▲) was measured relative to the amount of radioactivity remaining in the medium following the incubations (n=3 per time point). Uptake was linear with time and the net accumulation rate (K_i) was determined from the slope of the relevant regression equation. The data are summarized below each plot. Expression of the CD-UPRT fusion gene enabled cells to accumulate radiotracer at an increased rate as compared to CD-UPRT- cells. CD-UPRT+ cells incubated with [^{3}H]-5FU accumulated radiotracer at a rate that was an order of magnitude faster than that of CD-UPRT- cells. This accumulation rate was also substantially faster than that observed for CD-UPRT+ cells incubated with [^{14}C]-5FC. Moreover, the increase in accumulation for CD-UPRT+ cells incubated with [^{3}H]-5FU resulted in intracellular tracer levels that were a full log order higher than in CD-UPRT- cells (P=0.0043). CD-UPRT+ cells incubated with [^{14}C]-5FC demonstrated significant, while less dramatic, increases in radiotracer levels relative to CD-UPRT- cells (P=0.0014).

Supplementary Figure 2. Representative serial ^{19}FMR spectra of 5FU and anabolite FNuc in wild type (CD-UPRT-) (a) and transduced (CD-UPRT+) (b) subcutaneous xenografts. Spectral acquisition was initiated 7 minutes after i.v. injection of 5FU. The median time point relative to the time of injection is indicated for each spectrum. Western blots of ^{19}FMRS studied tumors demonstrating expression of the 22 41kD CD-UPRT protein corresponding to the spectral data are shown (c). Lane 1, CD-UPRT- tumor tissue, Lane 2, CD-UPRT+ tumor tissue. We implanted mice subcutaneously with either CD-UPRT+ or CD-UPRT- W256 cells and selected 175-250 mm^3 tumors for experiment (n = 5 per cohort). Following the intravenous (i.v.) injection of 150 mg/kg 5FU, its anabolism to FNuc was monitored by serial ^{19}F spectra in tumors (Supplementary Fig 1 a and b). The identification of 5FU and its FNuc metabolites was made based on documented chemical shifts[36, 37]. The intratumoral concentration of 5FU peaked in the initial spectrum and subsequently decreased rapidly for both tumor types. CD-UPRTtumors produced modest FNuc signals reaching an average peak concentration of only 1.24 ± 0.31 mM. In contrast, the intratumoral FNuc concentration in CDUPRT$^+$ rapidly reached a plateau, achieving an average concentration of 3.34 ± 0.27 mM, and decreased only slightly thereafter. These data demonstrate that 5FU is an effective probe for detecting the rapid accumulation of a marker metabolite (FNuc) specific for UPRT activity by ^{19}FMRS. The ^{19}FMRS data were validated through Western blot analysis performed following each experiment which confirmed that the expression of the CD-UPRT fusion gene was limited to the CD-UPRT+ tumors.

Supplementary Figure 3. Schematic representation of the bicistronic retroviral vector. The viral long terminal repeats (LTR) control expression of the *Saccharomyces cerevisiae* cytosine deaminase (yCDA)-*Haemophilus influenzae* uracil phosphoribosyltransferase (iUPP) fusion gene, while expression of the neomycin phosphotransferase (NEO) from the single transcript is mediated by an encephalomyocarditis virus derived internal ribosome entry site (IRES)[38]. The 23 coding sequences for yCDA (Erbs P et al. Curr Genet. 1997 Jan;31(1):1-6) and iUPP (Fleischmann RD et al. Science. 1995 Jul 28;269(5223):496-512) have been described previously and were linked by a glycine adaptor. Unique restriction sites used for cloning are indicated. Plasmid containing yCDA cDNA was kindly provided by Professor Brian Ross, University of Michigan. An iUPP encoding cosmid was obtained from ATCC (Rockville, MD).

Supplementary Figure 4. Plots showing impact of the different fixed values for the half saturation concentration of the FNuc to anabolites reaction, $K_{m,FNuc}$ used in the pharmacokinetic. (a) Plot of the final weighted residuals versus $K_{m,FNuc}$. The model produced virtually identical results for values of $K_{m,FNuc}$ less than about 100 μM, below which the rate equation describing the anabolism of FNuc is effectively zero order and therefore completely determined by $V_{max,5FU}^{FNuc}$. The fits became significantly worse for values of $K_{m,FNuc}$ above 100 μM only stabilizing when the rate equation effectively became linear at a $K_{m,FNuc}$ above about 420 mM. (b) Plot of the fit determined values for $V_{max,5FU}^{wt}$ (——) and $V_{max,5FU}^{UPRT}$ (– – –) versus $K_{m,FNuc}$. Both of these V_{max} values were largely independent of the value for $K_{m,FNuc}$ thus, any uncertainty in the precise value for $K_{m,FNuc}$ is of little consequence.